ARTICLES

Ultrafast Stimulated Emission and Structural Dynamics in Nickel Porphyrins

Xiaoyi Zhang,[†,‡] Erik C. Wasinger,[†] Ana Z. Muresan,[§] Klaus Attenkofer,[‡] Guy Jennings,[‡] Jonathan S. Lindsey,[§] and Lin X. Chen*[,†,||]

Chemistry Division and X-ray Science Division, Advanced Photon Source, Argonne National Laboratory, Argonne, Illinois 60439, Department of Chemistry, North Carolina State University, Raleigh, North Carolina 27695, and Department of Chemistry, Northwestern University, Evanston, Illinois 60208

Received: July 3, 2007; In Final Form: September 14, 2007

The excited-state structural dynamics of nickel(II)tetrakis(2,4,6-trimethylphenyl)porphyrin (NiTMP) and nickel-(II)tetrakis(tridec-7-yl)porphyrin (NiSWTP) in a toluene solution were investigated via ultrafast transient optical absorption spectroscopy. An ultrashort stimulated emission between 620 and 670 nm from the S_1 state was observed in both nickel porphyrins only when this state was directly generated via Q-band excitation, whereas such a stimulated emission was absent under B (Soret)-band excitation. Because the stimulated emission in the spectral region occurs only from the S_1 state, this photoexcitation-wavelength-dependent behavior of Ni(II) porphyrins is attributed to a faster intersystem crossing from the S_2 state than the internal conversion $S_2 \rightarrow S_1$. The dynamics of the excited-state pathways involving the (π, π^*) and (d, d) states varies with the meso-substituted peripheral groups, which is attributed to the nickel porphyrin macrocycle distortion from a planar configuration. Evidence for intramolecular vibrational relaxation within 2 ps and vibrational cooling in 6−20 ps of a (d, d) excited state has been established for NiTMP and NiSWTP. Finally, the lifetimes of the vibrationally relaxed (d, d) state also depend on the nature of the peripheral groups, decreasing from 200 ps for NiTMP to 100 ps for the bulkier NiSWTP.

Introduction

Metalloporphyrins have been extensively studied due to their resemblance to chromophores that play essential roles in biological processes, such as chlorophylls in natural photosynthetic reaction center proteins and antenna complexes,[1−5] heme groups in myoglobins and hemoglobins,[6−9] and cofactors in cytochrome P450 enzymes.[10−13] Among metalloporphyrins, Ni(II) porphyrins have been studied extensively because their versatile excited-state properties enable studies of fundamental photochemical processes including intersystem crossing, internal conversion, photoinduced axial ligation/deligation, as well as energy and charge transfer.[14−19]

UV−vis spectra of nickel porphyrins have a very intense B-band (Soret band) and a relatively weak Q-band corresponding to the respective transitions of $S_0 \rightarrow S_2$ and $S_0 \rightarrow S_1$ (where $S_{0,1,2}$ denotes the ground state and the lowest and the second lowest energy excited state), respectively. Both S_1 and S_2 involve MOs of predominantly porphyrin macrocycle character and are attributed to $^1(\pi, \pi^*)$ excited states. However, these excited states interact electronically with unfilled metal-centered MOs of d character via processes of energy transfer, electron shifting, and spin−orbit coupling, which are considered as possible routes for excited-state deactivation in metalloporphyrins with open-shell metals.[20,21] Previous studies on nickel porphyrins concluded that S_1 and S_2 decayed nonradiatively to the ground state via a Ni(II)-centered (d_{z^2}, $d_{x^2-y^2}$) state with lifetimes of 100−500 ps.[14,15,18,21,22] The (d_{z^2}, $d_{x^2-y^2}$) state, referred to as (d, d) hereafter, corresponds to a one-electron transfer from metal $3d_{z^2}$ to $3d_{x^2-y^2}$. The electronic configuration of this (d, d) state has been experimentally confirmed in nickel porphyrins by our recent X-ray transient absorption (XTA) spectroscopic studies, which showed an energy splitting of about 2.2 eV between the $3d_{z^2}$ and the $3d_{x^2-y^2}$ MOs.[23] Early studies on NiTPP [nickel(II)tetraphenylporphyrin] and NiOEP [nickel(II)octaethylporphyrin] wherein the Soret band was photoexcited revealed that the $^1(\pi, \pi^*)$ excited states evolved into the (d, d) state faster than the experiments could resolve at the time (i.e., 350 fs).[18,21,24] Drain et al. studied the excited-state dynamics of nickel(II)-dodecaphenylporphyrin (NiDPP) and nickel(II)tetra-*t*-butylporphyrin (Ni(*t*-Bu)P) in various solvents using ultrafast TA spectroscopy. The initial $^1(\pi, \pi^*)$ excited-state decay time constant was 0.7 ps for NiDPP and <0.5 ps for Ni(*t*-Bu)P. However, neither study reported the characteristic stimulated emission of the $^1(\pi, \pi^*)$ excited state following photoexcitation.[22,25]

The sub-picosecond $^1(\pi, \pi^*) \rightarrow (d, d)$ conversion and expected energy difference between these two states make it highly plausible that most of the excess energy after the conversion will be dissipated by intra- and intermolecular vibrational relaxation. Both transient absorption spectroscopy and time-resolved resonance Raman spectroscopy studies of

* Corresponding author. Tel.: (630) 252-3533; fax: (630) 252-9289; e-mail: lchen@anl.gov.
[†] Chemistry Division, Argonne National Laboratory.
[‡] X-ray Science Division, Advanced Photon Source, Argonne National Laboratory.
[§] North Carolina State University.
[||] Northwestern University.

10.1021/jp0751763 CCC: $37.00
Published on Web 10/30/2007

nickel porphyrins show that the (*d*, *d*) state undergoes a vibrational cooling process within 25 ps after photoexcitation and then decays to the ground state.[18,22,24,26−28] Studies by Kim et al. and Kitagawa and Mizutani proposed a dual-process model of the (*d*, *d*) state vibrational relaxation, in which the unrelaxed (*d*, *d*) state undergoes intramolecular vibrational relaxation (IVR) in approximately 0.5−2 ps and vibrational cooling (VC) in about 5−25 ps.[24,26,28]

In this study, we examined the excited-state dynamics of two other meso-tetrasubstituted nickel porphyrins, NiTMP [nickel-(II)meso-tetrakis(2,4,6-trimethylphenyl)porphyrin] and NiSWTP [nickel(II)meso-tetrakis(tridec-7-yl)porphyrin, or nickel tetra-"swallowtail" porphyrin] in toluene under both Q- and B-band excitation to induce the $S_0 \rightarrow S_1$ and $S_0 \rightarrow S_2$ transitions, respectively. These excited-state properties are compared to those of the previously studied NiTPP. We have examined the influence of peripheral groups on excited-state dynamics and decay pathways as well as on the structural dynamics. In a separate publication, structural dynamics of the excited state of NiTMP in toluene were investigated by XTA, where the electronic configuration and molecular geometry of the relaxed (*d*, *d*) state were directly determined.[23] Our optical TA results indicate that the excited-state dynamics varies between two meso-tetrasubstituted nickel porphyrins, NiTMP and NiSWTP. More interestingly, an ultrafast stimulated emission signal from the emitting S_1 state was captured within 1 ps after the S_1 state was directly excited. However, this ultrafast stimulated emission signal was not detected when the S_2 state was excited. Hence, the excitation-wavelength-dependent stimulated emission suggests a faster intersystem crossing from the S_2 state than the internal conversion $S_2 \rightarrow S_1$.

Materials and Methods

Choice of Compounds and Preparation. A key design criterion for the porphyrins to be examined in excited-state structural studies was a high solubility in organic solvents. The porphyrins chosen were meso-substituted porphyrins bearing four mesityl substituents or four symmetrically branched tridecyl (i.e., swallowtail) substituents; both porphyrins have higher solubilities in organic solvents such as toluene than porphyrins such as tetraphenylporphyrin. The two target nickel porphyrins bearing four mesityl (NiTMP) or swallowtail (NiSWTP) groups are shown in Figure 1. The free base porphyrins H_2TMP[29] and H_2SWTP[30] were synthesized according to published procedures. Several conditions were investigated for the nickel metalation of H_2TMP, employing metal salts such as $NiCl_2 \cdot 6H_2O$ and Ni(OAc)$_2 \cdot 4H_2O$ and various solvents (THF, $CHCl_3/CH_3OH$, and DMF) at room temperature or with heating. The nickel porphyrin NiTMP was obtained in 93% yield upon using excess Ni(OAc)$_2 \cdot 4H_2O$ in refluxing DMF for 24 h. Metalation of swallowtail porphyrin H_2SWTP proceeded smoothly using an excess of Ni(OAc)$_2 \cdot 4H_2O$ in hot $CHCl_3/CH_3OH$ (10:1) to give NiSWTP in 79% yield. Porphyrins NiTMP and NiSWTP were characterized by thin layer chromatography, absorption spectroscopy, fluorescence spectroscopy, ^{1}H NMR spectroscopy, and mass spectrometry (LD-MS and FAB-MS). In each case, fluorescence spectroscopy showed the absence of any contaminating free base porphyrin species. Experimental procedures and characterization data for NiTMP and NiSWTP are provided next. NiTPP was purchased from Frontier Scientific (Logan, UT) and used without further purification.

NiTMP. Following a reported procedure[31] with modification, a solution of free base meso-tetramesitylporphyrin (H_2TMP, 0.065 g, 0.083 mmol, 0.60 mM) in DMF (100 mL) was treated

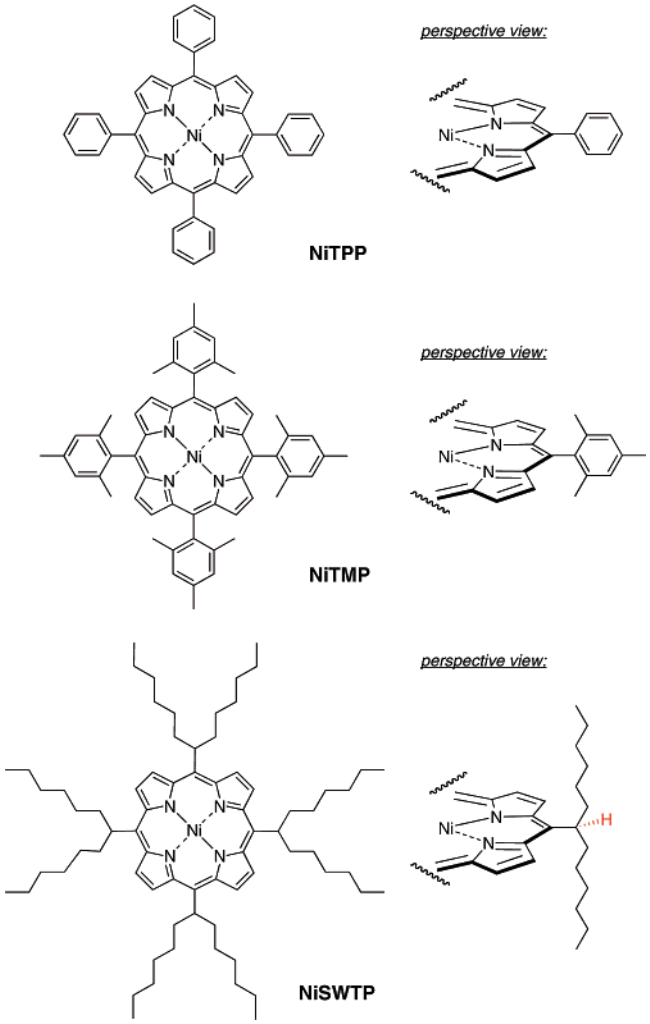

Figure 1. Structures of nickel porphyrins (left) and perspective views showing the porphyrin meso substituents (right). In NiSWTP, the hydrogen at the branch site (shown in red) lies in the plane of the macrocycle owing to the projection of the bulky alkyl groups.

with Ni(OAc)$_2 \cdot 4H_2O$ (0.826 g, 3.32 mmol). The heterogeneous mixture was stirred and refluxed under argon for 24 h. The reaction mixture was allowed to cool to room temperature. The mixture, containing the precipitated product, was concentrated under reduced pressure. The resulting solid residue was dissolved in CH_2Cl_2 and subsequently washed with water, $NaHCO_3$, and brine. The organic layer was separated, dried (Na_2SO_4), concentrated, and chromatographed [silica, hexanes/CH_2Cl_2, (1:1)]. The fraction containing the product was concentrated to give a purple solid. The solid was suspended in methanol. The suspension was sonicated and centrifuged. Decanting afforded the product as a solid pellet. This procedure was repeated twice whereupon the supernatant was colorless. The resulting solid was dried in vacuo, affording a crystalline orange−purple solid (0.064 g, 93%): ^{1}H NMR δ ($CDCl_3$, 400 MHz) 8.53 (s, 8H), 7.20 (s, 8H), 2.57 (s, 12H), 1.81 (s, 24H); LD-MS obsd 839.0; FABMS obsd 838.3574, calcd 838.3545 ($C_{56}H_{52}N_4Ni$); λ_{abs} (toluene) 415, 527 nm.

NiSWTP. A solution of free base meso-tetrakis(tridec-7-yl)-porphyrin (H_2SWTP, 0.035 g, 0.033 mmol) in $CHCl_3$ (10 mL) was treated with a solution of Ni(OAc)$_2 \cdot 4H_2O$ (0.167 g, 0.672 mmol) in CH_3OH (1 mL). The solution was stirred and refluxed under argon for 24 h. After cooling, water was added. The organic layer was separated, washed ($NaHCO_3$ and brine), dried (Na_2SO_4), and concentrated. The mixture was chromatographed

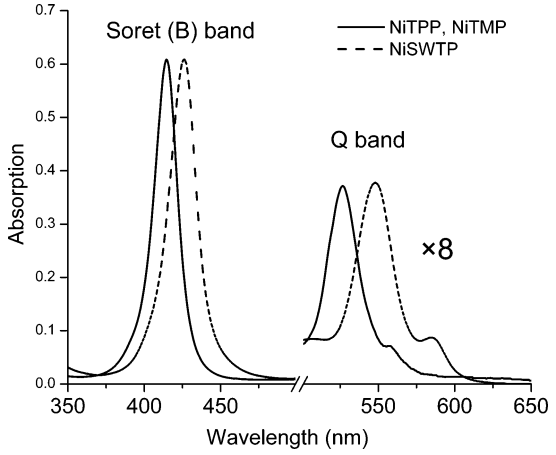

Figure 2. Ground-state absorption of nickel(II)porphyrins in toluene.

(silica, *n*-heptanes). The fast-moving fraction containing the product was concentrated to give a pink−purple solid (29 mg, 79%): ^{1}H NMR δ ($CDCl_3$, 400 MHz) 9.20 (s, 8H), 4.26−4.32 (m, 4H), 2.53−2.66 (m, 8H), 2.43−2.52 (m, 8H), 1.27−1.39 (m, 8H), 1.05−1.25 (m, 56H), 0.72−0.76 (m, 24H); LD-MS obsd 1094.8; FABMS obsd 1094.8563, calcd 1094.8553 ($C_{72}H_{116}N_4Ni$); λ_{abs} (toluene) 426, 547, 586 nm.

UV−vis Absorption Spectroscopy. The ground-state UV−vis spectra of the approximately 20 μM samples were recorded with a Shimadzu UV-2401PC spectrophotometer and 2 mm path length cuvettes.

Femtosecond Transient Absorption Spectroscopy. The ultrafast TA spectra were measured with a Ti:sapphire laser system with a regenerative amplifier and an optical parametric amplifier (OPA) as described elsewhere.[32] The concentrations of the samples were approximately 6×10^{-5} to 1.2×10^{-4} M. The optical pump pulses were either the second harmonic output of the Ti:sapphire amplifier at 418 nm or the output of the OPA. The white light generated by focusing a few microjoules of the Ti:sapphire amplifier output onto a sapphire disk was split into two beams for the probe and probe reference. The time-dependent TA signals at different pump and probe wavelengths were fit to a multiexponential function, convoluted with a Gaussian instrument response function of 120 fs fwhm. The multiexponential function, $f(t) = \sum_i A_i \exp(-t/\tau_i)$ commonly used in TA data analysis, was derived on the assumption of first-order reaction kinetics with parallel pathways from the first excited state. For a sequential pathway,

$$A \xrightarrow{k_1} B \xrightarrow{k_2} C...,$$

where k_i is the rate constant for step i, the multiexponential function can be expressed as $f(t) = A_1^0 e^{-t/\tau_1} + A_1^0 \tau_2 (\tau_2 - \tau_1)^{-1} (e^{-t/\tau_2} - e^{-\tau/\tau_1}) + ...$, where $\tau_i = 1/k_i$. The two models converge when the rate constants for consecutive reaction steps are well-separated (e.g., $k_2 \ll k_1$). For comparison, we used both parallel and sequential pathway models in the fitting. The sequential model fit consistently better for the fast components, while the value of the rate constants did not change significantly between fits with the two models.

Results and Discussion

Electronic Spectra of the Ground States. The ground-state UV−vis absorption spectra of NiTPP, NiTMP, and NiSWTP are shown in Figure 2. The UV−vis absorption spectra of NiTMP and NiTPP are almost identical, whereas the B- and Q-bands of NiSWTP in toluene are considerably red-shifted. The red-shifts in the B- and Q-bands relative to those of NiTPP and NiTMP suggest greater nonplanar distortion in NiSWTP, in accord with a previous study where a series of nickel porphyrins with various steric hindrances was examined.[33] The branched long alkyl chains at the meso positions in NiSWTP are bulkier than the phenyl groups in NiTPP and the mesityl groups in NiTMP, inducing a more nonplanar distortion. In addition, the B- and Q-bands in the spectrum of NiSWTP are slightly broader, and the Q(0, 0) band is more intense as compared to those corresponding features of NiTPP and NiTMP, also suggesting a more significant deviation from the planar conformation in NiSWTP than the other two. At the concentrations used for the TA measurements, no aggregation was observed because the band shape was independent of concentration, and the band intensities were proportional to the concentration.

Excitation-Wavelength-Dependent Stimulated Emission. A strong excitation-wavelength-dependence of the excited-state dynamics was observed in both NiTMP and NiSWTP. As shown in Figure 3A, transient absorption spectra of NiTMP within 0.6 ps after the laser pump pulse differ when the Q- and B-band are excited, respectively, by 527 and 418 nm light. A distinct dip near 630 nm appears as a negative TA signal overlaid with a typical broad S_1 excited-state absorption upon Q-band excitation at 527 nm. In contrast, the negative TA signal was absent upon B-band excitation. The kinetic traces probed at 630 nm with both excitation wavelengths (Figure 4A) further confirmed that this negative TA feature was only present for less than 0.6 ps when the S_1 state was directly generated through Q-band excitation at 527 nm. The negative TA signal was reproducible and repeatable. In addition, this negative feature was not observed with a blank toluene solvent. It is well-established that characteristic negative TA features of porphyrin TA spectra in the spectral region of 580−670 nm originate from the Q(0, 1) and Q(0, 0) bands of the stimulated emission from the S_1 or the lowest energy $^1(\pi, \pi^*)$ state.[18] For example, we measured TA spectra of ZnTPP (zinc-tetraphenylporphyrin) in toluene and observed two negative TA peaks (at 585 and 645 nm) corresponding to stimulated emission from the Q(0, 1) and Q(0, 0) bands of the S_1 state, respectively.[34] In addition, the main negative TA feature for NiTMP is near 630 nm, and that for NiSWTP is near 656 nm, which are consistent with their Q-band positions in the ground-state absorption spectra in Figure 2. Therefore, the negative TA feature in this spectral region upon Q-band excitation is evidently due to the emitting S_1 state. Other possibilities, such as ground-state bleaching and emission from other states, are ruled out because (a) there is no ground-state absorption in this region and (b) there are no known emitting states other than the lowest energy $^1(\pi, \pi^*)$ state that would emit in this spectral region.[18] The TA spectra of NiTMP and NiSWTP at 0.4 and 0.6 ps after the Q-band excitation are shown in Figure 3. Because of the spectral overlap between the stimulated emission and the excited-state absorption, their opposite TA signal polarities, and their comparable decay time constants that are close to the width of the instrumental response function (IRF) of 120 fs fwhm, it is challenging to extract the two time constants very accurately from our data. On the basis of our best fits of the experimental data, the lifetime of the S_1 state is in a range of 0.2−0.4 ps upon Q-band excitation of NiTMP with 527 nm light. The same excitation-wavelength-dependence of the negative TA signal with the same lifetimes was also observed in NiSWTP (Figures 3B and 4B).

When the B-band is excited, the emitting S_1 state can be generated only through the internal conversion $S_2 \rightarrow S_1$, which

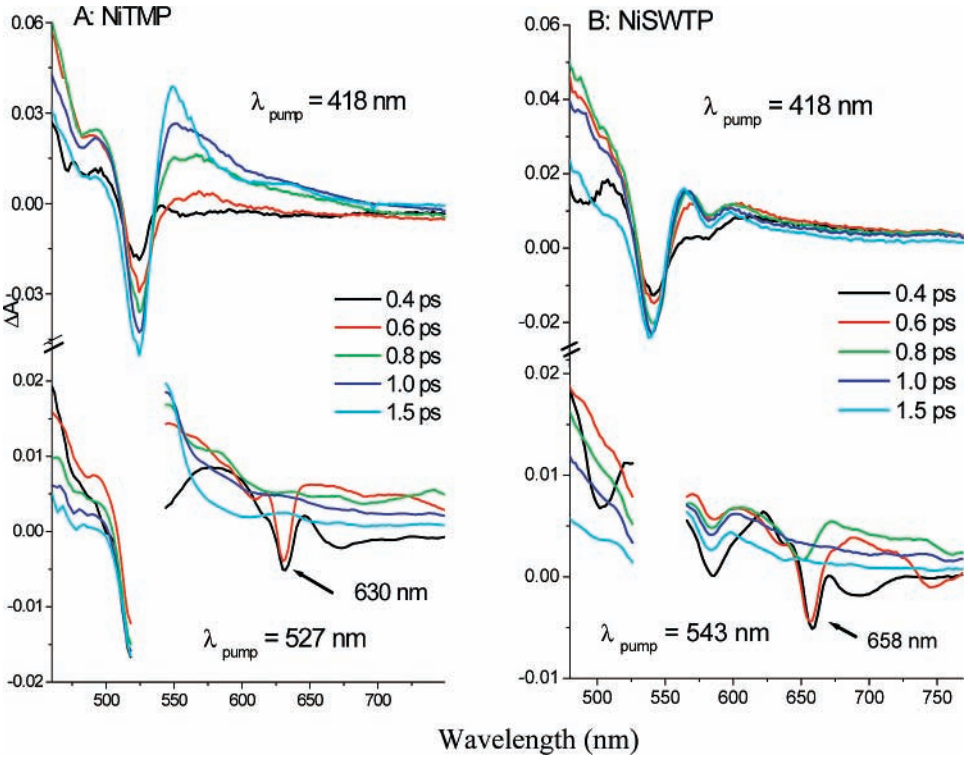

Figure 3. Transient absorption of (A) NiTMP and (B) NiSWTP in toluene at delay times between 0 and 1.5 ps after B-band (418 nm) and Q-band (527 nm for NiTMP and 543 nm for NiSWTP) excitation.

has been considered the main deactivation pathway of the S_2 state.[14,15,18,21,22,24] If this were the case, the stimulated emission from the S_1 state should be detected following the B-band excitation, which obviously is at odds with our experimental results. Thus, other excited-state decay pathways from the S_2 state must be considered, such as intersystem crossing to an upper triplet state followed by internal conversion to the lowest energy triplet state T_1. Our excitation-wavelength-dependent TA results suggest that the intersystem crossing from the S_2 state must be significantly faster than the internal conversion $S_2 \rightarrow S_1$. Hence, the emitting S_1 state population is only sufficient to allow detection upon direct generation by Q-band excitation. To confirm this assessment, we remeasured the TA spectra of NiTPP where the stimulated emission was not observed with the B-band excitation in previous studies.[18,24] Indeed, the same negative TA feature can be observed only with the Q-band excitation as that in NiTMP (Figure 4C). Evidently, the missing stimulated emission in NiTPP in previous studies was either due to the limited experimental time resolution or the spectral range at the time of the studies or that the studies were carried out with the B-band excitation only.

Vibrational Relaxation of the $^3(d, d)$ Excited State. Figure 5A displays TA spectra for NiTMP at delays from 1.5 to 400 ps after B-band (418 nm) and Q-band (527 nm) excitation. The TA spectra show bleaching of the Q-band ground state in the 500−530 nm region and excited-state absorption in the region of 460−500 nm and above 530 nm. The kinetic traces probed at discrete wavelengths in the 500−550 nm region following B-band excitation can be described by a triexponential function with time constants of $\tau_1 = 0.5-2$ ps, $\tau_2 = 13-20$ ps, and $\tau_3 = 190-210$ ps. The slowest decay process with $\tau_3 = 190-210$ ps has been attributed to the ground-state recovery from the vibrationally relaxed $^3(d, d)$ state. The absence of stimulated emission following the B-band excitation excludes any detectable contribution from the S_1 state. The lack of absorption in the 740−780 nm region rules out the presence of other possible intermediate states such as the $^3(\pi, \pi^*)$ and (d, π^*) states.[18] Thus, we can conclude that the S_2 state of NiTMP evolves into the hot (d, d) excited state faster than the experimental time resolution (<120 fs).

The TA spectrum of NiTMP under the B-band excitation in the first 1.5 ps (Figure 3A) shows a broad S_1 excited-state absorption band, which then becomes narrower and blue-shifted during the next 20 ps, while no new spectral features emerge. The time evolution of these spectral features is characteristic for the IVR and VC processes through which the excess energy generated from the rapid $^1(\pi, \pi^*) \rightarrow (d, d)$ conversion dissipates. The excess energies from the $^1(\pi, \pi^*) \rightarrow (d, d)$ conversion can be roughly estimated from the energies for $S_0 \rightarrow S_1$ and $S_0 \rightarrow S_2$ transitions and the energy required to induce a one-electron transition from $3d_{z^2}$ to $3d_{x^2-y^2}$ MOs. The B- and Q-band energies are 2.99 and 2.35 eV, respectively, but there is no precise value for the energy required to achieve a one-electron transition from $3d_{z^2}$ to $3d_{x^2-y^2}$. The latter process is not symmetry allowed but can be achieved via energy transfer through the $^1(\pi, \pi^*)$ state. Previously, the energy gap between $3d_{z^2}$ and $3d_{x^2-y^2}$ in the excited state came predominantly from calculations.[35] By contrast, this energy gap was directly measured in our recent XTA spectroscopy studies to be about 2.2 eV at the relaxed (d, d) state.[23] The broad excited-state absorption spectra in the short delay time originate from a vibrationally hot (d, d) excited state created upon the $^1(\pi, \pi^*) \rightarrow (d, d)$ conversion. Clearly, more excess energy is deposited on the molecule from B-band versus Q-band excitation. Consequently, the blue-shift and spectral narrowing are slower upon B-band excitation than those with Q-band excitation (Figure 5).

Figure 6 displays the kinetic traces of NiTMP within the first 18 ps following B-band excitation probed at three different wavelengths from the red to blue sides of the excited-state absorption peak. The rise of the blue side and the decay of the red side of the excited-state spectra reflect excited-state population redistribution among vibrational levels during the previously

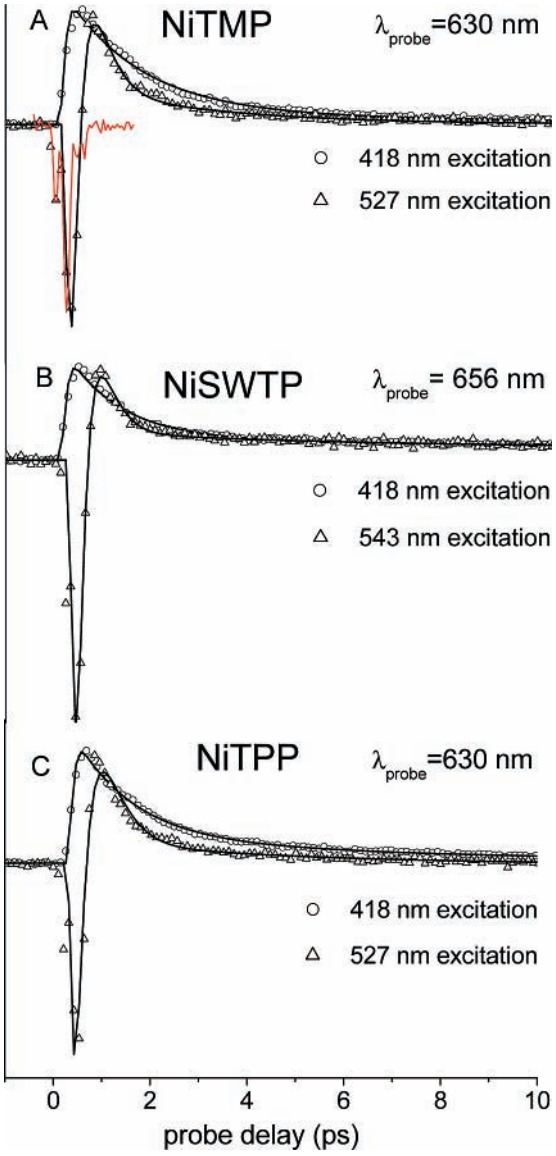

Figure 4. Transient absorption kinetics of Ni(II)-porphyrins in toluene (A) NiTMP, (B) NiSWTP, and (C) NiTPP. Multiexponential function fits are shown as black lines. Kinetic traces obtained with the B-band excitation were fit by a simple sum of the multiple exponential functions, whereas those with Q-band excitation were fit by both parallel and sequential reaction pathway models (see Materials and Methods). Fitting curves given by the two models are almost identical. Also included in panel A is the IRF in red with 120 fs fwhm.

mentioned IVR and VC processes. At 540 nm, which is on the blue side of the peak, the TA signal rises with two time constants, 1.4 and 18 ps, reflecting the IVR and VC processes before reaching an equilibrated (*d*, *d*) state. At 560 nm, which is on the red side of the peak, the TA signal increases almost instantaneously as the $^1(\pi, \pi^*)$ state rises and then decays with a similar time constant as those for the rise of the 540 nm signal. Therefore, the rise of the 540- nm signal and the decay of the 560 nm signal are highly correlated as expected for a vibrational relaxation process. As the excess energy redistributes among the vibrational levels, the population in the lower vibrational levels increases, resulting in a larger energy gap for the transition from T_1 to the upper excited states and hence the blue-shift in the excited-state absorption. Meanwhile, the population for the higher vibrational levels that are initially populated will decrease as a result of shifting the population to the lower vibrational levels. As the initial broad $^1(\pi, \pi^*)$ excited-state absorption evolves with time after the excitation, a sharpening to a distinctive peak occurs within 2 ps; continued narrowing and shifting to the blue occurred in the next 20 ps. Finally, the intensity of this peak decreases with a time constant of 200 ps as a result of the ground-state recovery. Thus, we attribute τ_1 to intramolecular energy redistribution among the vibrational modes of the (*d*, *d*) excited state and τ_2 to intermolecular energy redistribution through vibrational cooling by the solvent. The amplitudes of the two vibrational constants also agree with previous studies on other nickel porphyrins by Kim et al.[24] and by Kitagawa and Mizutani.[26−28] Kim et al. observed only one fast exponential decay in the spectral range of 460−500 nm for the excited-state kinetics of NiTPP in toluene, 0.6−0.7 ps in addition to the long ground-state recovery; however, they observed additional intermediate exponential decay components for NiTPP in pyridine and piperidine, ranging in 10−30 ps, which was attributed to the strong solute−solvent coupling.[24] We have revisited the kinetics of NiTPP in toluene and also observed only one fast component similar to the previous studies. Therefore, the intermediate time constant of 10−20 ps observed in the excited-state kinetics of NiTMP in toluene may indicate a stronger interaction of the molecule with the solvent that makes the vibrational cooling more pronounced and detectable. This assumption is in accord with a factor of >20 higher solubility of NiTMP than NiTPP in toluene, which makes NiTMP more soluble in toluene than NiTPP in pyridine.

The TA spectra of NiSWTP during 1.5−300 ps after B- and Q-band excitation are shown in Figure 5B. The kinetic data with B-band excitation are well-presented by a triexponential decay function with time constants of $\tau_1 = 0.1-0.5$ ps, $\tau_2 = 6-8$ ps, and $\tau_3 \approx 100$ ps. Similar to NiTMP, those three time constants are assigned to intramolecular vibrational relaxation, vibrational cooling, and the (*d*, *d*) excited-state decay to the ground state.

Fitting the kinetic data of NiTMP and NiTPP in toluene obtained with Q-band excitation results in similar vibrational time constants and (*d*, *d*) state lifetimes as those with B-band excitation. The excited-state dynamics of NiTMP and NiSWTP based on our studies are summarized in Figure 7.

Effects of meso-Tetrasubstituted Groups on Electronic Structure. In comparison with the TA spectra of NiTMP in toluene, those for NiSWTP in toluene show (a) a less pronounced blue-shift of the excited-state absorption, (b) shorter excited-state decay time constants, and (c) broader TA spectra at delay times longer than 1.5 ps. In addition, the overall profiles of the TA spectra for NiTMP and NiSWTP are significantly different from one another. For example, NiSWTP has clearly visible ground-state bleaching of the Q(0, 0) band at 580 nm, whereas NiTMP has almost no visible ground-state bleaching of the Q(0, 0) band in the TA spectra (Figure 4). This is in agreement with the ground-state absorption spectra of the two complexes shown in Figure 2, where NiSWTP shows a more intense Q(0, 0) band absorption relative to that of NiTMP. Moreover, the excited-state Q-band absorption of NiSWTP is much broader than that of NiTMP. There are two possible explanations for the broadened excited-state absorption of NiSWTP: more severe nonplanar distortion and conformational heterogeneity.

Ni(II) in the low spin ground state has a smaller radius than the coordination cavity of the porphyrin macrocycle. Hence, the coordination between Ni(II) and N atoms in the pyrrole rings will pull the entire macrocycle to accommodate shorter Ni(II)−N distances, resulting in nonplanar distortions. When $^3(d, d)$ is formed upon photoexcitation of the Ni(II) porphyrin, electron

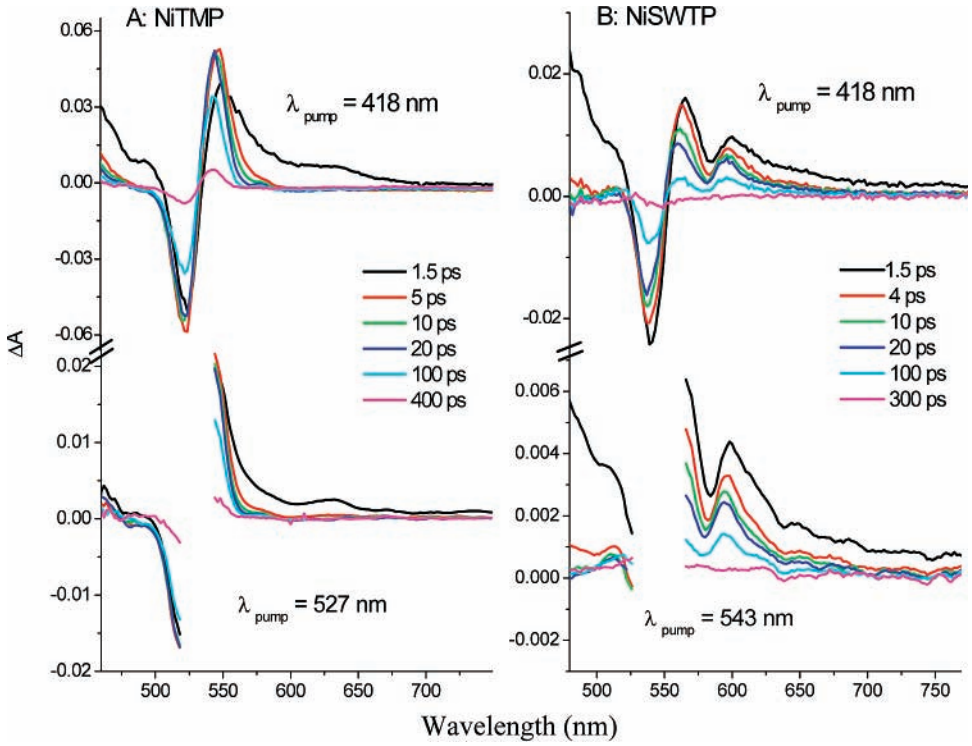

Figure 5. Transient absorption of (A) NiTMP and (B) NiSWTP in toluene at delay times between 1.5 and 400 ps after B-band (418 nm) and Q-band (527 nm for NiTMP and 543 nm for NiSWTP) excitation.

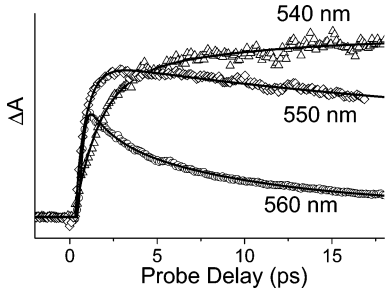

Figure 6. Transient absorption kinetics of NiTMP in toluene probed at different wavelengths in the first 18 ps after B-band excitation.

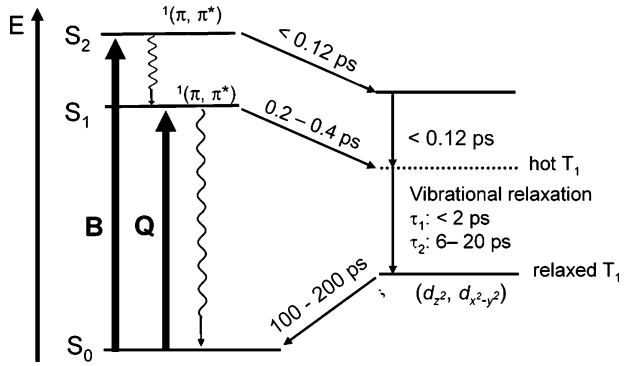

Figure 7. Excited-state relaxation pathway of NiTMP and NiSWTP with an experimental time resolution of about 0.12 ps.

repulsion between the $3d_{x^2-y^2}$ orbital and the macrocycle in the $^3(d, d)$ state induces an effective expansion of the Ni radius, thereby resulting in a more planar structure than that in the ground state. Such a macrocycle expansion of the $^3(d, d)$ state has been directly measured by our recent XTA study of NiTMP in toluene, showing the elongation of the average Ni−N and Ni−C_α distances in the T_1 excited state by 0.08 and 0.07 Å, respectively, relative to the ground-state structure.[23] It is conceivable from the XTA results that the T_1 state of NiTMP is more planar than the ground state as the Ni−N bonds become longer. In this regard, the normal-coordinate structural decomposition analysis and molecular dynamics calculations by Shelnutt et al. also showed that the nonplanar deformations decreased as four-coordinating Ni(II) meso-tetrasubstituted porphyrins switched from low spin to high spin,[36] just as in the T_1 state. Therefore, longer Ni−N distances and a flatter macrocycle are the preferred configuration for the high spin T_1 state. Because of the steric hindrance imposed by the bulky swallowtail groups at the meso positions, the flattening of the T_1 state for NiSWTP would be less significant. Therefore, the T_1 excited state of NiSWTP may still have significant nonplanar distortion, which on one hand destabilizes the excited state and on the other hand results in a less pronounced blue-shift and spectral narrowing than that of NiTMP. This also explains the shorter T_1 excited-state lifetime for NiSWTP (100 ps) versus that of NiTMP (200 ps).

For alkyl-substituted nickel porphyrins, calculations indicate that the energy barriers between the lowest energy ruffled (or $\alpha\beta\alpha\beta$) conformation and other conformations in the excited state are significantly smaller as compared to those in the ground state.[36,37] For phenyl-substituted nickel porphyrins, such as NiTPP, in contrast, calculations suggested that the potential surface in the excited state preferred a single nearly planar conformation.[16,36] Thus, it would be easier for the T_1 state of an alkyl-substituted nickel porphyrin to adopt multiple nonplanar conformations and to sample a larger energy landscape than that for the ground state. Consequently, there would be diverse pathways for vibrational relaxation, resulting in broad excited-state absorption spectra. In comparison, NiTMP, which closely resembles NiTPP, is expected to have a narrow distribution of excited-state structures with a nearly planar conformation, resulting in a less broad excited-state absorption spectrum.

Conclusion

The excited-state dynamics of the meso-substituted porphyrins NiTMP and NiSWTP were studied using ultrafast TA spec-

troscopy. Strong excitation-wavelength-dependent stimulated emission has been observed in NiTMP, NiSWTP, and NiTPP. The $^1(\pi, \pi^*)$ excited state can be spectrally resolved only if molecules are directly excited to the S_1 state and the lifetime of the S_1 excited state is 0.2−0.4 ps for all three nickel porphyrins. We propose that intersystem crossing in the S_2 state is faster than the internal conversion of $S_2 \rightarrow S_1$. Both NiTMP and NiSWTP exhibit dual-process decays in the vibrational relaxation of the (*d*, *d*) excited state: an IVR process within 2 ps and a VC process with a time constant of 6−20 ps. The TA spectrum time evolution of NiSWTP shows significantly less blue-shift and narrowing than that of NiTMP. This difference is attributed to a more nonplanar distortion and more accessible conformations of the (*d*, *d*) excited state of NiSWTP.

Acknowledgment. The work was supported by the U.S. Department of Energy, Office of Science, Office of Basic Energy Sciences under Contracts DE-AC02-06CH11357 (Argonne National Laboratory) and DE-FG02-96ER14632 (North Carolina State University). We thank Prof. Dewey Holten for insightful discussions.

References and Notes

(1) Joran, A. D.; Leland, B. A.; Felker, P. M.; Zewail, A. H.; Hopfield, J. J.; Dervan, P. B. *Nature (London, U.K.)* **1987**, *327*, 508.
(2) Khundkar, L. R.; Perry, J. W.; Hanson, J. E.; Dervan, P. B. *J. Am. Chem. Soc.* **1994**, *116*, 9700.
(3) Portela, C. F.; Brunckova, J.; Richards, J. L.; Schollhorn, B.; Iamamoto, Y.; Magde, D.; Traylor, T. G.; Perrin, C. L. *J. Phys. Chem. A* **1999**, *103*, 10540.
(4) Sakata, Y.; Tsue, H.; Oneil, M. P.; Wiederrecht, G. P.; Wasielewski, M. R. *J. Am. Chem. Soc.* **1994**, *116*, 6904.
(5) Wuttke, D. S.; Bjerrum, M. J.; Winkler, J. R.; Gray, H. B. *Science (Washington, DC, U.S.)* **1992**, *256*, 1007.
(6) Ashkenasy, G.; Ivanisevic, A.; Cohen, R.; Felder, C. E.; Cahen, D.; Ellis, A. B.; Shanzer, A. *J. Am. Chem. Soc.* **2000**, *122*, 1116.
(7) Godbout, N.; Sanders, L. K.; Salzmann, R.; Havlin, R. H.; Wojdelski, M.; Oldfield, E. *J. Am. Chem. Soc.* **1999**, *121*, 3829.
(8) Rose, E.; Lecas, A.; Quelquejeu, M.; Kossanyi, A.; Boitrel, B. *Coord. Chem. Rev.* **1998**, *180*, 1407.
(9) Zhang, X. M.; Tong, M. L.; Gong, M. L.; Lee, H. K.; Luo, L.; Li, K. F.; Tong, Y. X.; Chen, X. M. *Chem.—Eur. J.* **2002**, *8*, 3187.
(10) Groves, J. T. *J. Porphyrins Phthalocyanines* **2000**, *4*, 350.
(11) Meunier, B.; Bernadou, J. *Metal-Oxo and Metal-Peroxo Species in Catalytic Oxidations*; Springer-Verlag: Berlin, 2000; Vol. 97, p 1.
(12) Ogliaro, F.; de Visser, S. P.; Groves, J. T.; Shaik, S. *Angew. Chem., Int. Ed.* **2001**, *40*, 2874.
(13) Yang, J.; Gabriele, B.; Belvedere, S.; Huang, Y.; Breslow, R. *J. Org. Chem.* **2002**, *67*, 5057.
(14) Kim, D.; Holten, D. *Chem. Phys. Lett.* **1983**, *98*, 584.
(15) Kim, D.; Kirmaier, C.; Holten, D. *Chem. Phys.* **1983**, *75*, 305.
(16) Jentzen, W.; Unger, E.; Karvounis, G.; Shelnutt, J. A.; Dreybrodt, W.; Schweitzer-Stenner, R. *J. Phys. Chem.* **1996**, *100*, 14184.
(17) Song, X.-Z.; Jentzen, W.; Jaquinod, L.; Khoury, R. G.; Medforth, C. J.; Jia, S.-L.; Ma, J.-G.; Smith, K. M.; Shelnutt, J. A. *Inorg. Chem.* **1998**, *37*, 2117.
(18) Rodriguez, J.; Holten, D. *J. Chem. Phys.* **1989**, *91*, 3525.
(19) Chen, L. X.; Jaeger, W. J. H.; Jennings, G.; Gosztola, D. J.; Munkholm, A.; Hessler, J. P. *Science (Washington, DC, U.S.)* **2001**, *292*, 262.
(20) Zamyatin, A. V.; Soldatova, A. V.; Rodgers, M. A. J. *Inorg. Chim. Acta* **2007**, *360*, 857.
(21) Rodriguez, J.; Holten, D. *J. Chem. Phys.* **1990**, *92*, 5944.
(22) Drain, C. M.; Kirmaier, C.; Medforth, C. J.; Nurco, J.; Smith, K. M.; Holten, D., *J. Phys. Chem.* **1996**, *100*, 11984.
(23) Chen, L. X.; Zhang, X.; Wasinger, E. C.; Attenkofer, K.; Jennings, G.; Musresan, A. Z.; Lindsey, J. S. *J. Am. Chem. Soc.* **2007**, *129*, 9616.
(24) Eom, H. S.; Jeoung, S. C.; Kim, D.; Ha, J.-H.; Kim, Y.-R. *J. Phys. Chem. A* **1997**, *101*, 3661.
(25) Drain, C. M.; Gentemann, S.; Roberts, J. A.; Nelson, N. Y.; Medforth, C. J.; Jia, S.; Simpson, M. C.; Smith, K. M.; Fajer, J.; Shelnutt, J. A.; Holten, D. *J. Am. Chem. Soc.* **1998**, *120*, 3781.
(26) Mizutani, Y.; Kitagawa, T. *Bull. Chem. Soc. Jpn.* **2002**, *75*, 623.
(27) Mizutani, Y.; Kitagawa, T. *Bull. Chem. Soc. Jpn.* **2002**, *75*, 965.
(28) Mizutani, Y.; Kitagawa, T. *J. Mol. Liq.* **2001**, *90*, 233.
(29) Lindsey, J. S.; Wagner, R. W. *J. Org. Chem.* **1989**, *54*, 828.
(30) Thamyongkit, P.; Lindsey, J. S. *J. Org. Chem.* **2004**, *69*, 5796.
(31) Tsurumaki, H.; Watanabe, Y.; Morishima, I. *Inorg. Chem.* **1994**, *33*, 4186.
(32) Greenfield, S. R.; Wasielewski, M. R. *Opt. Lett.* **1995**, *20*, 1394.
(33) Haddad, R. E.; Gazeau, S.; Pecaut, J.; Marchon, J. C.; Medforth, C. J.; Shelnutt, J. A. *J. Am. Chem. Soc.* **2003**, *125*, 1253.
(34) Du, H.; Fuh, R.-C. A.; Li, J.; Corkan, L. A.; Lindsey, J. S. *Photochem. Photobiol.* **1998**, *68*, 141.
(35) Patchkovskii, S.; Kozlowski, P. M.; Zgierski, M. Z. *J. Chem. Phys.* **2004**, *121*, 1317.
(36) Song, Y. J.; Haddad, R. E.; Jia, S. L.; Hok, S.; Olmstead, M. M.; Nurco, D. J.; Schore, N. E.; Zhang, J.; Ma, J. G.; Smith, K. M.; Gazeau, S.; Pecaut, J.; Marchon, J. C.; Medforth, C. J.; Shelnutt, J. A. *J. Am. Chem. Soc.* **2005**, *127*, 1179.
(37) Song, X.-Z.; Jentzen, W.; Jia, S.-L.; Jaquinod, L.; Nurco, D. J.; Medforth, C. J.; Smith, K. M.; Shelnutt, J. A. *J. Am. Chem. Soc.* **1996**, *118*, 12975.